Astronomy & Astrophysics

FIRST-based survey of Compact Steep Spectrum sources

II. MERLIN and VLA observations of medium-sized symmetric objects

M. Kunert-Bajraszewska[1], A. Marecki[1], P. Thomasson[2], and R. E. Spencer[2]

[1] Toruń Centre for Astronomy, N. Copernicus University, 87-100 Toruń, Poland
e-mail: amr@astro.uni.torun.pl

[2] Jodrell Bank Observatory, The University of Manchester, Macclesfield, Cheshire SK11 9DL, UK

Abstract. A new sample of candidate Compact Steep Spectrum (CSS) sources that are much weaker than the CSS source prototypes has been selected from the VLA FIRST catalogue. MERLIN "snapshot" observations of the sources at 5 GHz indicate that six of them have an FR II-like morphology, but are not edge-brightened as is normal for Medium-sized Symmetric Objects (MSOs) and FR IIs. Further observations of these six sources with the VLA at 4.9 GHz and MERLIN at 1.7 GHz, as well as subsequent full-track observations with MERLIN at 5 GHz of what appeared to be the two sources of greatest interest are presented. The results are discussed with reference to the established evolutionary model of CSS sources being young but in which not all of them evolve to become old objects with extended radio structures. A lack of stable fuelling in some of them may result in an early transition to a so-called coasting phase so that they fade away instead of growing to become large-scale objects. It is possible that one of the six sources (1542+323) could be labelled as a prematurely "dying" MSO or a "fader".

Key words. radio continuum: galaxies – galaxies: active – galaxies: evolution

1. Introduction

It is intriguing that the range of linear sizes of FR II-type (Fanaroff & Riley 1974) double-structured radio sources is very large and spans from tens of parsecs to megaparsecs. For this and practical reasons FR II-like radio sources have been roughly divided into three classes: Compact Symmetric Objects (CSOs) – those with Largest Angular Sizes (LAS) below 1 h^{-1} kpc, Medium-sized Symmetric Objects (MSOs) with subgalactic sizes (LAS < 20 h^{-1} kpc) and Large Symmetric Objects (LSOs) – LAS ≥ 20 h^{-1} kpc (Fanti et al. 1995)[1]. Although the MSO class has been defined solely on morphological features without particular stress on the spectral properties of its members (Augusto et al. 1998), many of the sources (if not the majority) have steep spectra and consequently they have also been classified as Compact Steep Spectrum (CSS) sources. It would also appear that MSOs (which are unbeamed CSS sources) have similar morphologies to LSOs and that the lobe expansion velocities in CSOs are high enough for the rapid evolution of CSOs to MSOs (Owsianik & Conway 1998; Owsianik et al. 1998).

Readhead et al. (1996) proposed an evolutionary sequence unifying these three classes of radio-loud AGNs (RLAGNs) having morphological similarity but with different linear sizes. Snellen et al. (1999, 2000) discussed many aspects of the above scenario in detail. In particular, they concluded that the radio luminosity of a CSO increases as it evolves, reaches a maximum in the MSO phase and then gradually decreases as the object increases in size to become an LSO. The amount of time the source spends in each of these stages also increases: CSOs are younger than $\sim 10^4$ years, MSOs are typically $\sim 10^5$ years old and LSOs can manifest their activity for up to $\sim 10^8$ years. The ages of CSOs have been estimated from kinematic age arguments – see e.g. Polatidis & Conway (2003) for a review – whereas for larger sources, i.e. MSOs (Murgia et al. 1999) and LSOs (Alexander & Leahy 1987; Liu et al. 1992), spectral ages have been estimated.

The lobes of a large-scale RLAGN are huge reservoirs of energy – the minimum energy stored in the lobes is $\sim 10^{60}$ to 10^{64} erg (see e.g. Richstone et al. 1998) – so even if the energy supply from the central engine to the hotspots and the lobes eventually cuts off, the radio source should still be observable for a substantial period of time. As the source gradually fades, its spectrum becomes steeper and steeper because of radiation and expansion losses. This so-called "coasting phase" of the lobes of a RLAGN, which can last up to 10^8 years (Komissarov & Gubanov 1994; Slee et al. 2001), provides

---

[1] For consistency with earlier papers in this field, the following cosmological parameters have been adopted throughout this paper: $H_0 = 100$ km s^{-1} Mpc^{-1} and $q_0 = 0.5$. Wherever in the text we refer to linear sizes we introduce h^{-1}.

information on past nuclear activity. LSOs possessing these features are sometimes termed "faders" and, although relatively rare, have been observed, mostly in surveys of ultra-steep spectrum sources (Röttgering et al. 1994; De Breuck et al. 2000). B2 0924+30 is a good example of this and Cordey (1987), in describing the structure and properties of this double radio source as a possible relic radio galaxy with a projected linear size of 270 h^{-1} kpc, has indicated that the source is a "dying" LSO object. Recently, Jamrozy et al. (2004) have confirmed that B2 0924+30 is in fact a relic radio structure associated with an E/S0 galaxy, IC 2476, that "switched off" its activity $\sim 5 \times 10^7$ years ago and as such can be labelled a "dead" radio galaxy. The evolving spectra of the radio relics believed to be remnants of powerful radio galaxies have been studied by Goldshmidt & Rephaeli (1994) and Kaiser & Cotter (2002).

A question that naturally arises is whether the activity periods of galaxies can be much shorter than those pertinent to the LSOs. Intuitively, the answer to this question might be positive and Reynolds & Begelman (1997) – hereafter RB97 – have proposed a model in which extragalactic radio sources are intermittent on timescales of $\sim 10^4 - 10^5$ years. According to RB97, when the power supply cuts off, the radio emission fades rapidly. However, the shocked matter continues to expand supersonically and keeps the basic source structure intact. Thus, this model predicts that there should be a large number of MSOs that are weaker than those currently known, because of this power cut-off, and which should have steep spectra with no sign of active nuclei. If medium-scale, i.e. subgalactic-scale, faders could be found, then the theory developed by RB97 would be strongly supported. Looking for "weak" MSOs might also lead to the establishment of a more complete evolutionary scheme for radio sources in which a number of them do not follow the whole evolutionary track proposed by Readhead et al. (1996) but leave it at the MSO stage.

A search for medium-sized faders was one of the reasons for the establishment and observation of a sample of weak CSS sources using, as a basis, the early results from the *Faint Images of Radio Sky at Twenty cm* (FIRST) survey (White et al. 1997)[2]. A number of possible MSOs were identified and in this paper, the second in a series covering observations of the initial sample, the results of MERLIN and VLA observations of those sources considered to be weak MSOs are presented.

2. The parent sample and its previous observations

During the period following the publication of the very first paper defining a class of CSS sources (Peacock & Wall 1982) up to the year 2000, only two almost identical surveys of CSS sources (Spencer et al. 1989; Fanti et al. 1990), which were based upon the 3CR catalogue (Bennett 1962) and the Peacock & Wall (1982) list, have been used in investigations of the whole class. More recently a major step towards weaker sources has been made by Tschager et al. (2003) and earlier by Fanti et al. (2001) who carried out VLA observations of

candidate sources selected from the B3-VLA (Vigotti et al. 1989) survey. It became clear to us that the FIRST survey, because of its resolution (5″.4) and its low sensitivity limit, could contain many weak CSS sources. Using an early release of FIRST covering a strip of sky defined by right ascension in the range $7^h 30^m < \alpha < 17^h 30^m$ and declination in the range $28° < \delta < 42°$ we selected a flux density limited, complete sample consisting of ~60 candidate sources fulfilling the basic criteria of the CSS class: steep spectra between ~0.4 GHz and 5 GHz and high compactness. A detailed description of the selection criteria was given in Kunert et al. (2002) – hereafter Paper I. The candidates were, of course, much weaker than other known objects selected in a similar manner; their 5-GHz fluxes listed in the GB6 survey (Becker et al. 1991) were in the range 150 mJy $< S_{5\,GHz} <$ 550 mJy. Our sample is therefore at a comparable depth to that of Fanti et al. (2001).

The sample was initially observed with MERLIN in "snapshot" mode at 5 GHz (a "pilot" survey), the details of which, including typical $u - v$ coverage for the sources, were given in Paper I. Final images of five arcsecond-scale sources were also presented in Paper I, only one of which was a MSO with conspicuous hotsposts embedded within its FR II-like structure. Many of the images acquired in the pilot survey showed the need for follow-up observations of selected groups of objects using, appropriately, the VLA, MERLIN, the EVN and the VLBA. Six sources were identified as MSOs and potential candidates for scaled-down versions of faders. They appeared to be unaffected by beaming and Doppler boosting and had simple, double structures typical for MSOs, yet without clear indications of hotspots. The MERLIN 5-GHz "snapshot" images of these six MSOs are presented in Fig. 1. The details and results of further observations of these six sources with MERLIN and the VLA are also presented in this paper (Paper II). Observations of 19 other sources with angular sizes below 1″, many of them made using VLBI techniques, will be presented in a forthcoming paper (Paper III).

3. Follow-up observations and their reduction

It was realised that the 5-GHz MERLIN snapshot images of the pilot survey might have suffered from an undersampling of the $u - v$ plane and therefore some flux could be missing. To overcome this problem, the sources were observed with the VLA in A-configuration at 4.9 GHz. MERLIN 1.7-GHz observations were also made in an attempt to determine the spectral indices of the lobes.

The VLA observations at 4.9 GHz (0″.4 resolution) were carried out on 29 and 30 June 2003 in "snapshot" mode. Each target source was observed four times in 4-min scans interleaved with 1-min scans on phase calibrators. 3C 286 was used as a primary flux density calibrator and the whole data reduction process was carried out in AIPS using the standard phase and amplitude calibration tasks. The task SCMAP, initialised for a few passes of phase self-calibration, was used to produce "naturally weighted" images. The total intensity images are shown in Figs. 2a–f (left panels).
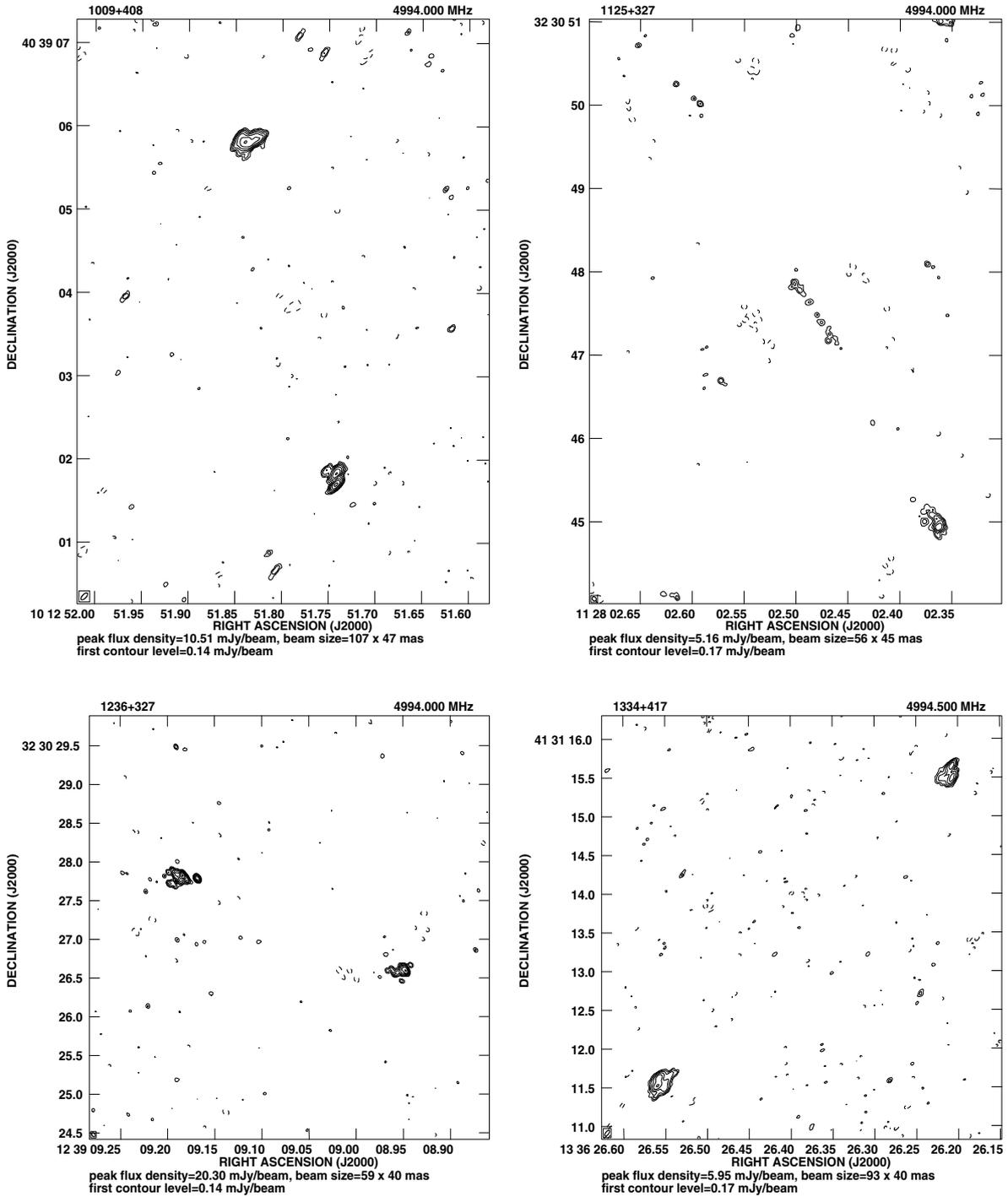

Fig. 1. MERLIN maps at 5 GHz resulting from "snapshot" observations (the "pilot" survey). Contours increase by a factor 2 and the first contour level corresponds to $\approx 3\sigma$.

The 1.7-GHz MERLIN observations (resolution $\sim 0\rlap{.}''15$) were carried out in February and March 2003. Each target source scan was interleaved with a scan on a phase reference source throughout an ~ 14-h track, except for the two sources 1236+327 and 1334+417. The total cycle time (target – phase-reference) was 6 min including telescope drive times, with ~ 3.5 min actually on the target source per cycle.

The increased sensitivity of MERLIN resulting from the inclusion of the Lovell telescope in the observations of 1236+327 and 1334+417 meant that both these sources and their associated phase-references could be interleaved at 1-h intervals in a single ~ 14-h track. The phase-reference sources were chosen from the MERLIN calibrator lists derived from the JVAS survey (Patnaik et al. 1992; Browne et al. 1998;
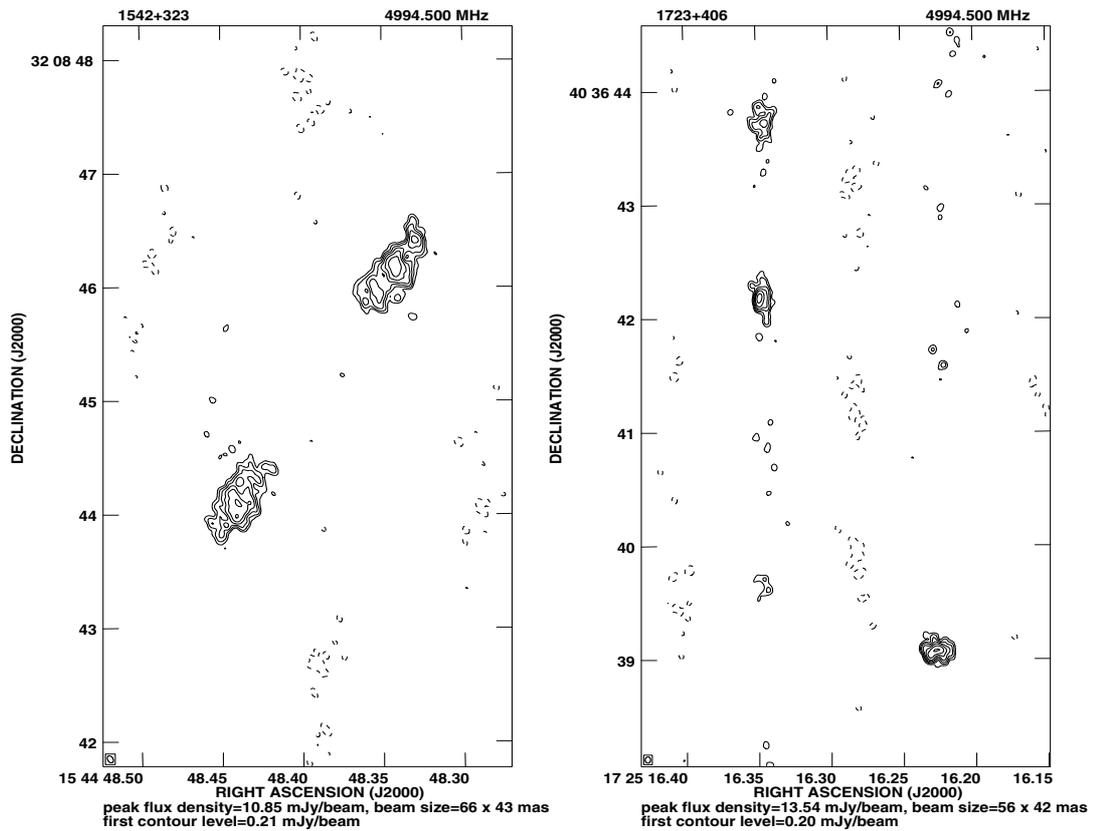
Fig. 1. continued.

Wilkinson et al. 1998). OQ208 was used as the point source or baseline calibrator and 3C 286 as the flux and polarisation calibrator. The flux density for 3C 286 at 1658 MHz on the VLA scale, which was used, was 13.639 Jy.

The initial editing and both amplitude and polarisation calibration of the data were carried out using the Jodrell Bank d-programmes and PIPELINE automated procedure. Further cycles of phase self-calibration and imaging using the AIPS tasks CALIB and IMAGR were then used to produce the final total power and, where available, the polarisation images shown in Figs. 2a–f (right panels).

The snapshot images of 1236+327 and 1542+323 showed that both sources deserved further investigation. Consequently, MERLIN full-track, phase-referenced observations of them were carried out on 18 and 24 May 2004 at 5 GHz and 4.9 GHz respectively. The high fidelity images resulting from these observations, as well as combined MERLIN+VLA images, are shown in Figs. 3 and 4.

The rms noise levels in the MERLIN 1.7-GHz images are significantly greater than in the VLA 4.9-GHz ones. The shortest MERLIN $u - v$ spacing is also only 12 km, which limits its sensitivity to more extended emission. Consequently, for both of the above reasons, attempts to produce detailed spectral index images from the MERLIN 1.7-GHz and VLA 4.9-GHz images, particularly in the regions of low-level extended emission, were unsatisfactory and the results have not been included.

The positions of the optical identifications of the sources, if available, extracted either from the POSS plates using the Automatic Plate Measuring (APM) machine or Third Data Release of the Sloan Digital Sky Survey (SDSS/DR3) are marked with crosses on the radio images.

In addition to the observations described above, an unpublished 8.4-GHz VLA observation of 1009+408 made by Patnaik et al. (1992) as part of the Jodrell Bank–VLA Astrometric Survey (JVAS) has been included here as this may be helpful in the presentation of our ideas (Fig. 2a – lower panel; Table 2).

The basic properties of the 6 sources are given in Table 1. Except for 1125+327 whose redshift estimate and linear size are commented upon in Sect. 4, the redshifts of the sources are unknown at the present time. The estimated total fluxes at 1.7 GHz quoted in Table 1 have been derived from an interpolation between the 1.4 GHz and 4.85 GHz fluxes assuming a constant spectral index. These values can provide an assessment of the missing flux in the MERLIN 1.7 GHz images when compared with a summation of the fluxes of the main components in the MERLIN images.

The flux densities of the components (or well defined features) of the sources at both 1.7 GHz and 4.9 GHz were measured using the AIPS task JMFIT and their spectral indices calculated. The results are listed in Table 2.

Table 1. Optical magnitudes derived form POSS plates using the APM and radio flux densities of 6 CSS sources at 1.4 and 4.85 GHz.

Source Name	RA h m s	Dec ° ′ ″	ID	m_R	Total flux at 1.4 GHz mJy	Total flux at 4.85 GHz mJy	$\alpha_{1.4\,\mathrm{GHz}}^{4.85\,\mathrm{GHz}}$	Total flux at 1.7 GHz mJy	LAS ″
(1)	(2)	(3)	(4)	(5)	(6)	(7)	(8)	(9)	(10)
1009+408	10 12 51.795	40 39 03.73	G	20.40	411	194	−0.60	366	4.06
1125+327	11 28 02.464	32 30 46.70	G	19.11	600	205	−0.86	508	6.81
1236+327	12 39 09.090	32 30 27.45	EF	–	832	256	−0.95	692	3.12
1334+417	13 36 26.394	41 31 13.37	G	22.62	470	154	−0.90	395	5.47
1542+323	15 44 48.395	32 08 45.11	G	21.14	854	325	−0.78	734	2.41
1723+406	17 25 16.268	40 36 41.38	EF	–	962	221	−1.18	765	4.65

Description of the columns:

- Col. (1): source name in the IAU format;
- Col. (2): source right ascension (J2000) extracted from FIRST;
- Col. (3): source declination (J2000) extracted from FIRST;
- Col. (4): optical identification: G-galaxy, EF-empty field;
- Col. (5): red magnitude;
- Col. (6): total flux density at 1.4 GHz extracted from FIRST;
- Col. (7): total flux density at 4.85 GHz extracted from GB6;
- Col. (8): spectral index ($S \propto \nu^\alpha$) between 1.4 and 4.85 GHz calculated using flux densities in Cols. (6) and (7);
- Col. (9): estimated total flux density at 1.7 GHz interpolated from data from Cols. (6) and (7);
- Col. (10): largest Angular Size (LAS) in arcseconds as estimated in the present paper.
        (LAS is measured as a separation between the outermost components' peaks.)

4. Comments on individual sources

1009+408. MERLIN and VLA images of this double source are shown in Figs. 1 and 2a. The more extended emission between the two main lobes seen in the 4.9-GHz VLA image is barely visible in the MERLIN 1.7-GHz image probably because of a lack of short spacings in the MERLIN data at 1.7 GHz. The only indication of a core in any of the images is in the 4.9-GHz VLA image, in which there is a peak of emission at RA = $10^h12^m51^s\!.82$, Dec = +40°39′04″.18, although even this is very doubtful as there is no indication of a core at this position in the MERLIN 5-GHz image. However, its determined Gaussian model parameters are given in Table 2. Crosses on the radio images indicate the position of a galaxy found using the SDSS/DR3. The northern lobe does not show any very compact features in any of the images and its spectral index is moderately steep. There is a hotspot at the edge of the southern lobe in both the 5-GHz MERLIN images and in the 8.4-GHz VLA image. There is also an asymmetry in polarisation between the lobes (Fig. 2a).

1125+327. MERLIN and VLA images of this double source are shown in Figs. 1 and 2b. A published VLA image of this radio galaxy at 1.46 GHz by Machalski & Condon (1983) showed it to have a triple structure with two bright components and one very weak one to the south-west of those two. As our MERLIN images at a similar frequency showed only a double structure with no south-western component, the raw 1.46-GHz data for this source originally used by Machalski & Condon (1983) was extracted from the VLA archive and reprocessed. No third component to the south-west was found and

so it is assumed that this component in the original 1.46-GHz VLA image is an artefact.

There is an intensity peak in the 4.9-GHz VLA image at RA = $11^h28^m02^s\!.44$, Dec = +32°30′46″.54 (Table 2), which may be a radio core. There is no such feature in the 1.7-GHz MERLIN image (Fig. 2b) so the core could have a flat or inverted spectrum as one might expect. Crosses on the radio images indicates the position of a galaxy found on the POSS plates using the APM. Machalski (1998) published a photometric redshift for this object: $z = 0.75$. However, it is to be noted that the position listed by Machalski (1998) is somewhat different from that in POSS which, together with the limited accuracy of the method, makes the redshift determination rather insecure. Bearing this in mind, but assuming the above quoted redshift, a linear extent of 27.6 h^{-1} kpc has been calculated which slightly exceeds the formal limit of the MSO class.

The extended emission visible in the VLA 4.9-GHz image is resolved out by MERLIN and consequently a large fraction (50%) of the flux in the 1.7-GHz image is missing. Also, ~10% of the flux in the 4.9-GHz VLA image has not been accounted for in the process of fitting the Gaussian components listed in Table 2 – this missing flux can be attributed to the diffuse bridge-like part of the NE lobe.

The southern lobe has two small peaks, one of which seems to be a hotspot as indicated by the 5-GHz MERLIN image (Fig. 1). The NE lobe is also edge-brightened by a flat spectrum hotspot.

1236+327. Following the analysis of the initial MERLIN and VLA observations of 1236+327 (Figs. 1 and 2c), it was
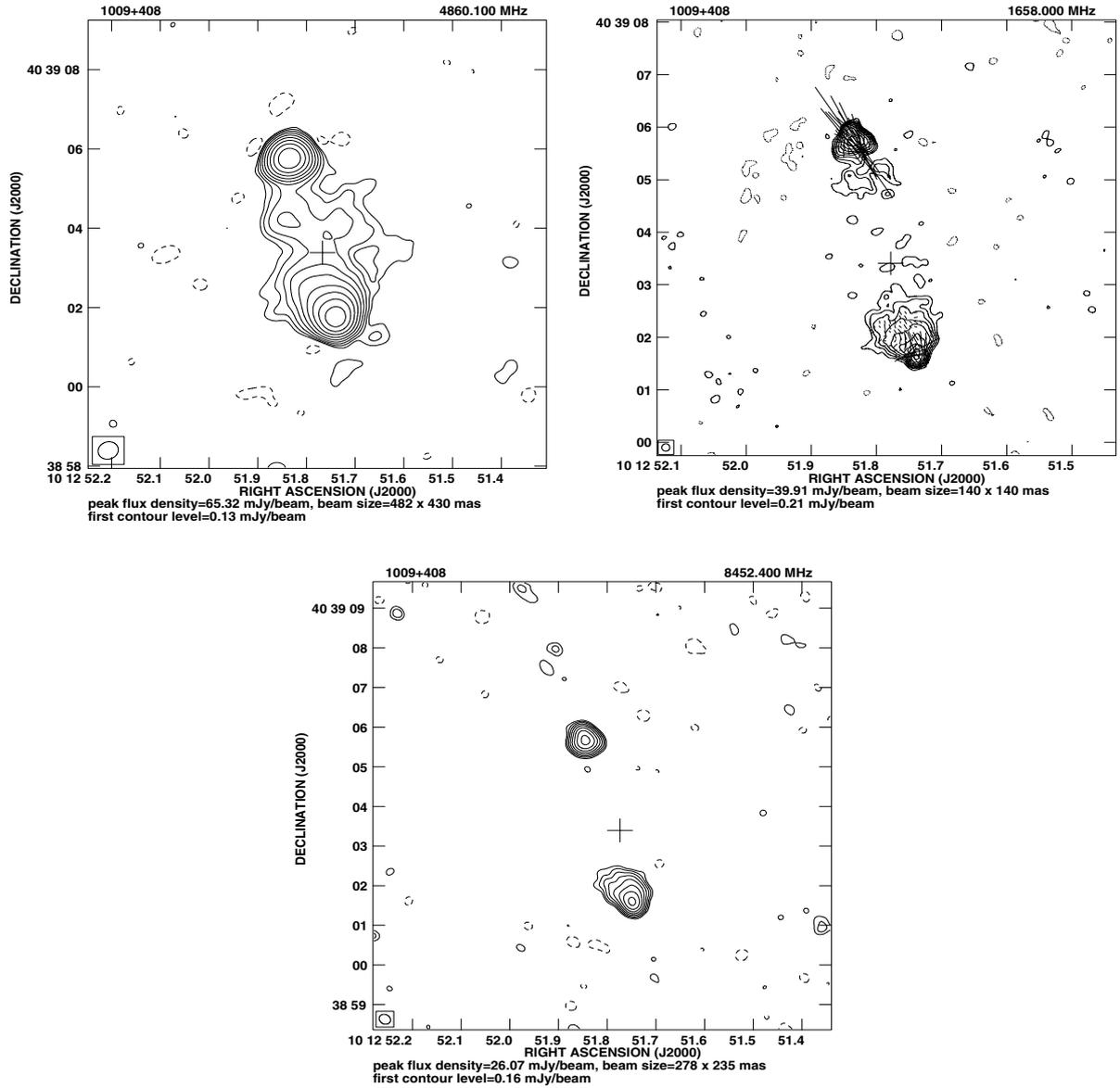
Fig. 2a. VLA map of 1009+408 at 4.9 GHz (*upper left*), MERLIN 1.7-GHz polarisation map (*upper right*) and VLA 8.4-GHz map (*lower*). Contours increase by a factor 2 and the first contour level corresponds to $\approx 3\sigma$. Polarisation line of 1″ amounts to 3.3 mJy/beam. Crosses indicate the position of an optical object found using the SDSS/DR3.

thought that the source might have a mixed morphology with the SW end clearly in an "active" phase, but the NE end possibly fading out. Similar cases of such sources have been described by Lonsdale & Morison (1983). They investigated sources with asymmetric structures and their research revealed that in each source, one hotspot is more compact and of less steep spectrum than its counterpart on the opposite side of the source. They divided hotspots into two different classes and postulated that class II hotspots are aged and expanded versions of class I hotspots. If the energy supply to a class I hotspot is removed, a steepening of the spectrum, an increase in size and a possible tangling of the magnetic field are to be expected. If there is a "working" jet supplying the lobe, the magnetic field lines have a tendency to lie perpendicular to the source axis.

In order to determine more fully the structure of 1236+327, a full-track MERLIN observation at 5 GHz was made. The resulting image is shown in Fig. 3 with the lower panels showing the polarised emission of the two lobes of the source in more detail. This full-track 5-GHz MERLIN data were also combined with the existing VLA 4.9-GHz data to produce the image also shown in Fig. 3 (upper right panel). It can be seen that the SW lobe has a comparatively simple, classical FR II type of structure, whereas the NE lobe appears to be very complex with several possible hotspots. It is to be noted that one can draw an almost perfect straight line between the western hotspot in the NE lobe, the peak of emission located at RA = $12^h39^m09^s.13$, Dec = +32°30′27″.6 and the hotspot in the SW lobe, indicating that this peak of emission between the two lobes is perhaps the core. Assuming this to be the case means that the source
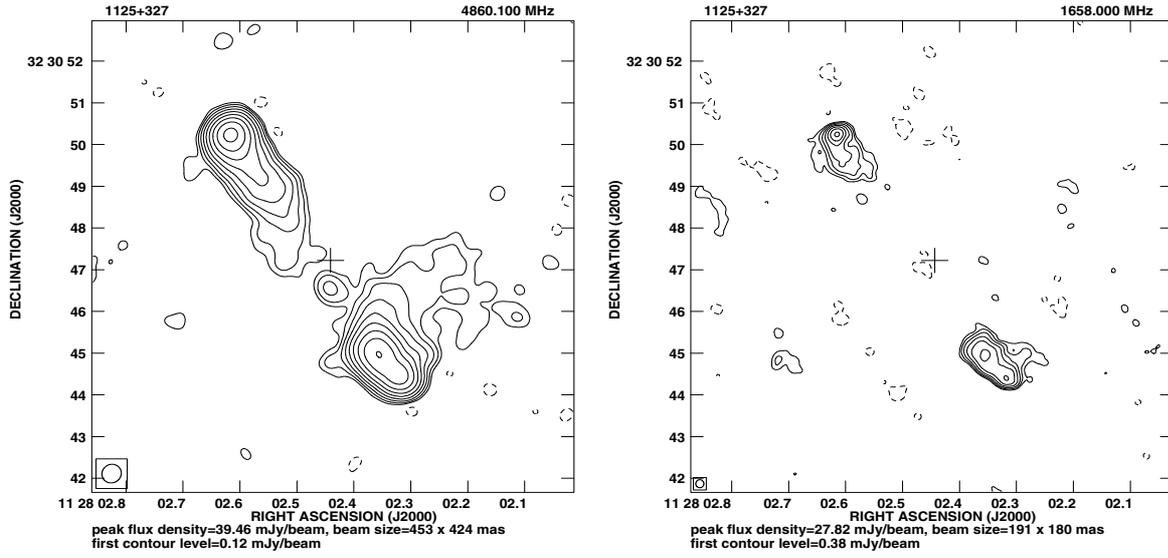
Fig. 2b. VLA map of 1125+327 (*left*) at 4.9 GHz and MERLIN map at 1.7 GHz (*right*). Contours increase by a factor 2 and the first contour level corresponds to ≈3σ. Crosses indicate the position of an optical object found on the POSS plates using the APM.
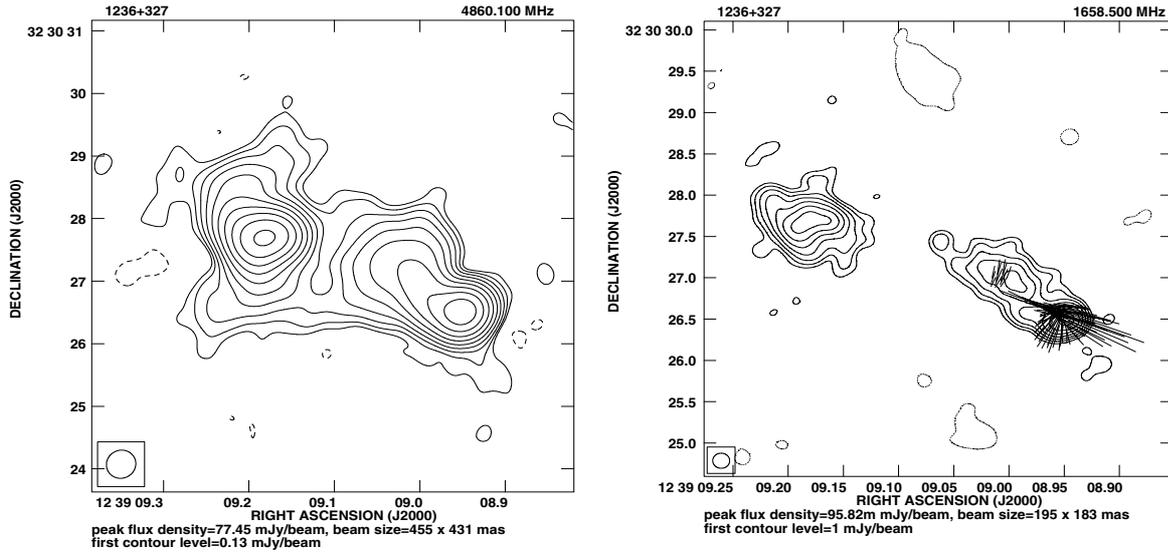

Fig. 2c. VLA map of 1236+327 at 4.9 GHz (*left*) and MERLIN polarisation map at 1.7 GHz (*right*). Contours increase by a factor 2 and the first contour level corresponds to ≈3σ. Polarisation line of 1″ amounts to 8.34 mJy/beam.

has a highly asymmetric arm ratio for its two lobes (~5.4), which is even larger than the value of ~5 quoted for 3C 459 by Thomasson et al. (2003).

Best et al. (1995) showed that the structures of FR II sources are probably determined by relativistic, environmental and intrinsic asymmetries. According to Arshakian & Longair (2000) relativistic effects are more important for quasars and high luminosities, whereas intrinsic/environmental asymmetries are more important for low luminosities and radio galaxies, and are more significant on small physical scales. The asymmetry in the structure of 1236+327 is probably caused by both orientation on the sky and interaction with the surrounding medium whereas the conjecture that this source might have

a mixed morphology with one lobe in an active phase, and another one possibly fading (Lonsdale & Morison 1983) is ruled out.

1334+417. This source has a classical double structure with two edge-brightened radio lobes (Figs. 1 and 2d). The southern lobe has a steep spectrum and the polarisation is detectable only in this lobe. The bridge of emission between the two lobes, clearly visible in the VLA 4.9 GHz image, is resolved out in the MERLIN 1.7 GHz image. As the flux emitted by the bridge contributes significantly to the total flux at both frequencies, the sum of the fluxes of the fitted Gaussians listed in Table 2 is far less than the total flux indicated in Table 1. Overall, the source
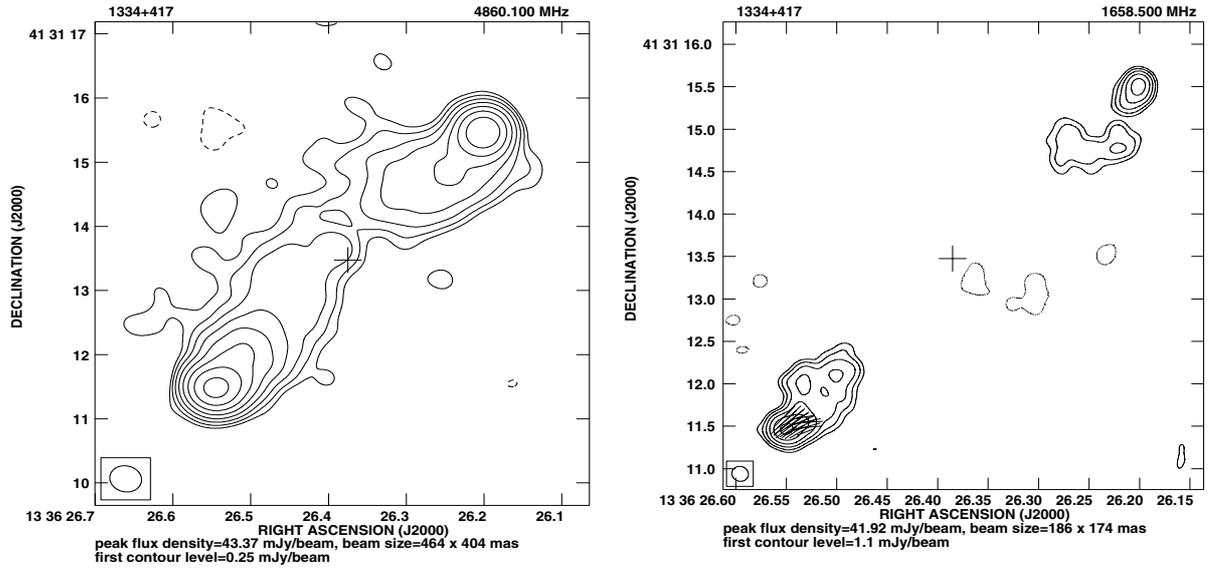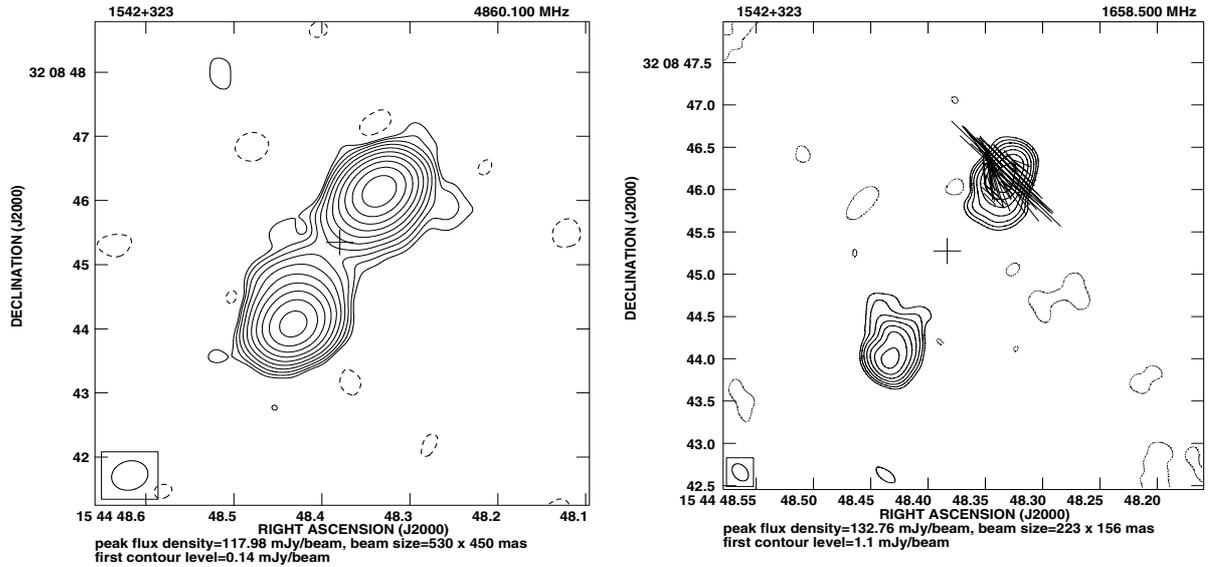
Fig. 2d. VLA map of 1334+417 at 4.9 GHz (*left*) and MERLIN polarisation map at 1.7 GHz (*right*). Contours increase by a factor 2 and the first contour level corresponds to ≈3σ. Polarisation line of 1″ amounts to 6.25 mJy/beam. Crosses indicate the position of an optical object found using the SDSS/DR3.

Fig. 2e. VLA map of 1542+323 at 4.9 GHz (*left*) and MERLIN polarisation map at 1.7 GHz (*right*). Contours increase by a factor 2 and the first contour level corresponds to ≈3σ. Polarisation line of 1″ amounts to 6.25 mJy/beam. Crosses indicate the position of an optical object found using the SDSS/DR3.

has a typical FR II-like morphology i.e. its lobes are clearly edge-brightened.

1542+323. The initial MERLIN and VLA images (Figs. 1 and 2e) indicated that this source might indeed be a fader. It did not appear to have a core, nor did the lobes, which were not edge-brightened, appear to have hotspots (Fig. 2e).

A full-track MERLIN observation at 4.86 GHz, the same frequency as the VLA observation, was made in order to more fully investigate the source lobe structure and to search for a core. The resulting images of the overall structure of the source

and the individual lobes including polarisation vectors on an enlarged scale are shown in Fig. 4. There is still no indication of a core or hotspots. It is to be noted that there is no change in the direction of the polarisation vectors (i.e. magnetic field) in the regions of maximum intensity, which one might expect if they were active hotspots. It would appear that this source could be a fader.

1723+406. MERLIN and VLA images of this double source are shown in Figs. 1 and 2f. This is clearly a triple source with an interesting bent structure in all our images. There
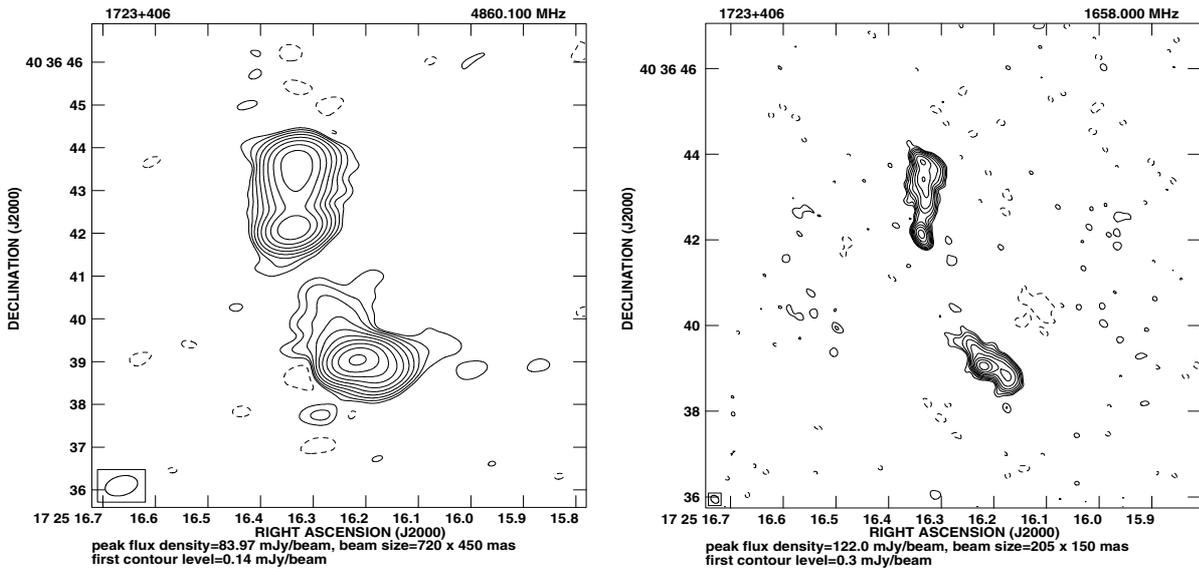
Fig. 2f. VLA map of 1723+406 at 4.9 GHz (*left*) and MERLIN map at 1.7 GHz (*right*). Contours increase by a factor 2 and the first contour level corresponds to ≈3σ.

appears to be a core, part of a jet and a radio lobe, although all these three components have very steep spectra, which possibly indicates that the true core is still hidden. Our 5-GHz MERLIN observations (Fig. 1) resolved out the extended emission visible in the 4.9-GHz VLA image and in the 1.7-GHz MERLIN image (Fig. 2f) so only two compact components show up: a core and probably a hotspot from the southern lobe and some diffuse emission from the jet. The radio structure of the source on the two sides of the nucleus exhibits different Fanaroff-Riley morphologies. Sources of that kind are called HYbrid MOrphology Radio Sources (HYMORS; Gopal-Krishna & Wiita 2000).

5. Discussion

Feretti et al. (1984) found a significant correlation between the core luminosity of radio galaxies P_c and the total radio power P_t (core + extended structure), but there was quite a large dispersion in this correlation. Also, over 30% of their sample only had upper limits for the core luminosities, which could have been due to a lack of observational sensitivity. Consequently, Giovannini et al. (1988) made much greater sensitivity observations with the VLA at 4.9 GHz of those sources whose cores had not been detected. A conclusion of their work was that two of their sources, whose cores were still undetected at a level which was at least two sigma below the expected $P_c - P_t$ correlation, could represent "dying" sources, i.e. the sources in which the supply of energy from the nucleus had ceased. A further four sources with $P_c - P_t$ approximately one sigma below the expected correlation were also probably "dying" sources.

The MERLIN 5-GHz image of 1542+323 (Fig. 4) shows two radio lobes without visible hotspots and without a core, the upper limit to the flux density of the latter being below that expected from the correlation of core luminosity at 4.9 GHz (log P_c) vs. total luminosity at 408 MHz (log P_t) for

all but the most powerful of radio galaxies (Giovannini et al. 1988 – Eq. (1)). (The source total flux density at 408 MHz (1.99 Jy) was estimated using a spectral index between 1.4 GHz and 365 MHz of −0.69, the latter being calculated from the 1.4-GHz flux given in Table 1 and the flux density at 365 MHz quoted in the Texas catalogue, Douglas et al. 1996.) Thus, it would appear that 1542+323 is possibly a CSS/MSO fader. However, although the above indicates that there is no longer a power supply from a central engine, the polarised emission in the northern lobe, in which there would appear to be no or very little Faraday rotation and depolarisation, indicates a measure of doubt about this.

The flux density ratios of the lobes of sources in the sample have been determined to see if there are any asymmetries, as it has already been noticed that in MSOs large lobe flux density asymmetries sometimes exist. It has also been postulated that most CSS sources may pass through a phase of evolution in an asymmetric environment (Saikia et al. 2001, 2002). There is only a small asymmetry in the flux densities of the lobes of our sources at the level of ~1.3.

A number of theoretical predictions of the existence of a class of young sources which never grow to large sizes have appeared recently. For example, Ghisellini et al. (2004) have suggested a model of aborted jets. In this model, the jets in a radio-quiet object could be accelerated to relativistic speeds and the object would thus become radio-loud. Eventually, when the active period comes to an end, diffuse, weak radio lobes without visible jets should be seen.

In interpreting the results of our observations, and 1542+323 in particular, the scenario proposed by RB97 could be adopted, namely that the energy supply from the jets might be interrupted. Taking into consideration the predictions made by RB97, it would appear that the evolutionary track of RLAGNs proposed by Snellen et al. (1999, 2000) is not necessarily the only one. In fact, they themselves admit that it is
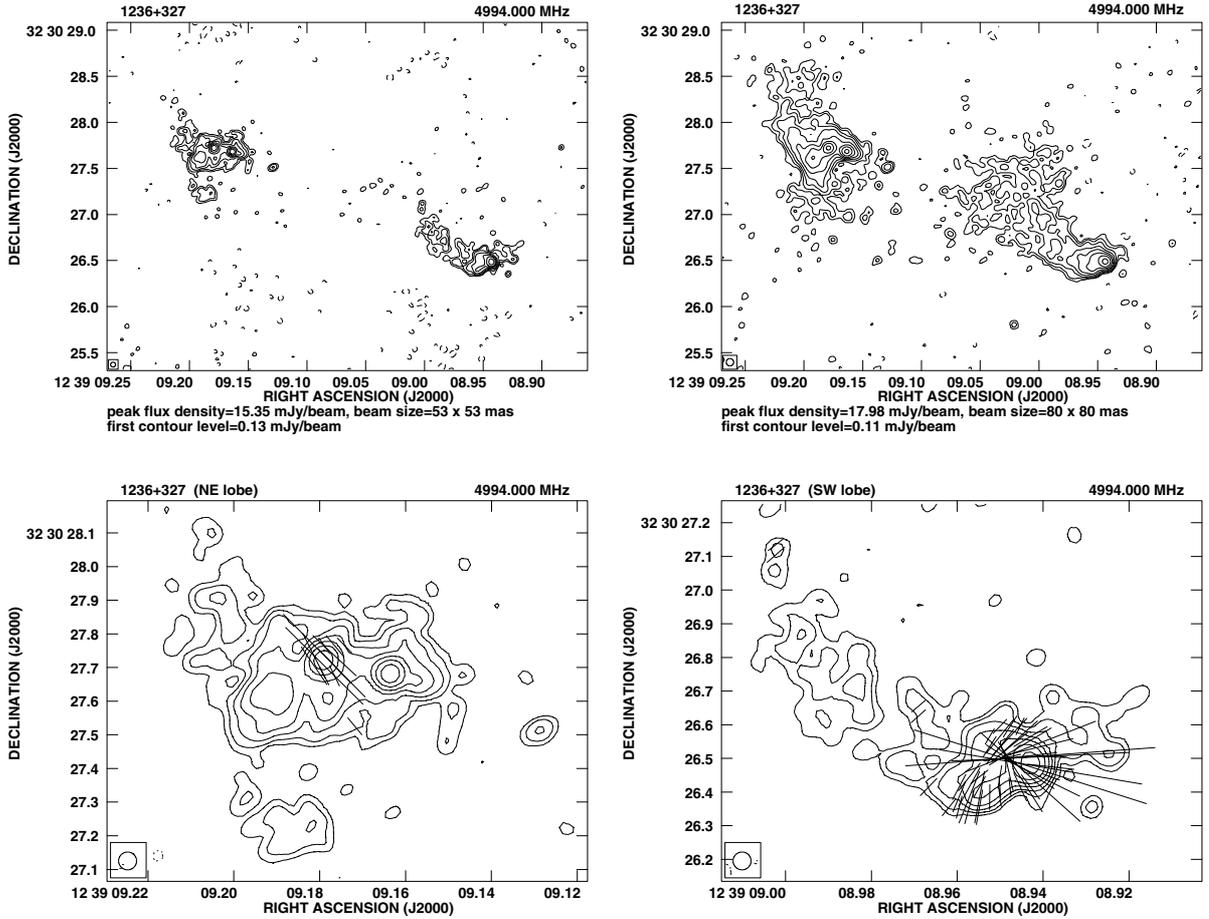
Fig. 3. MERLIN map of 1236+327 resulting from 12-h observation at 5 GHz (*upper left*). Combined MERLIN and VLA polarisation map of 1236+327 at 5 GHz (*upper right*). Lower panels show enlarged lobes of MERLIN-only map. Contours increase by a factor 2 and the first contour level corresponds to ≈3σ. Polarisation line of 1″ amounts to 3.33 mJy/beam for all maps.

unclear whether all young sources evolve into LSOs, and their plot shows an additional branch indicating sources which have left the "main sequence" at an earlier stage. (They labelled them "drop-outs".) Thus, a whole family (a continuum?) of such tracks might exist and the one shown by Snellen et al. (1999) appears as the *only* one simply because of a selection effect related to the Malmquist bias.

Therefore, the following scenario might be considered. Suppose the energy supply from the central engine cuts off after e.g. ~10^5 years i.e. a timescale typical for the spectral ages of CSS/MSOs (Murgia et al. 1999). Under such circumstances a "dying" CSS source would result which, provided it is not beamed towards us, would be perceived as an MSO. Just as for large-scale faders, a "dying" MSO, unlike a standard, high radio luminosity MSO, should be relatively weak because of a lack of fuelling and should not be edge-brightened because there are no (or hardly any) jets pushing through the intergalactic medium. Thus, the hotspots should have faded away. What should be seen therefore is nothing more than diffuse lobes without well defined hotspots analogous to those observed in large-scale faders.

The major problem with accepting the above scenario is that LSO faders should have very steep spectra (cf. Komissarov & Gubanov 1994), which is not the case for 1542+323: it has a mean spectral index of $\alpha = -0.78$ – see Tables 1 and 2. However, if it is assumed that expansion losses dominate in subgalactic-scale faders and that they could occur in a comparatively short period of time – 10^4 years (J.P. Leahy, priv. comm., but see also RB97), then the morphological signs of fading and a decrease in luminosity would take precedence over the transformation of the spectrum into a very steep one. Thus, the lobes would quickly take the typical form of a fader without their spectra showing signs of ageing for frequencies below 5 GHz. Thus, 1542+323 could still be labelled as a "fader".

Finally, the issue of the "unification" of small and large-scale faders should be discussed. It appears fairly obvious that a single mechanism should be at work in faders regardless of their sizes. The simplest reason for cessation of activity of an AGN is that there is no more matter to be accreted onto a Supermassive Black Hole (SMBH) in a host galaxy centre. An interesting alternative to that scheme, namely the mechanism of thermal-viscous instabilities in the accretion disk of an AGN,

Table 2. Flux densities of sources principal components at 1.7 GHz and 4.9 GHz.

Source Name	RA h m s	Dec ° ′ ″	$S_{1.7\,GHz}$ mJy	$S_{4.9\,GHz}$ mJy	$\alpha_{1.7\,GHz}^{4.9\,GHz}$	$S_{8.4\,GHz}$ mJy	$\alpha_{4.9\,GHz}^{8.4\,GHz}$	θ_1 ″	θ_2 ″	PA °
(1)	(2)	(3)	(4)	(5)	(6)	(7)	(8)	(9)	(10)	(11)
1009+408	10 12 51.83	40 39 05.74	154.81	85.39	−0.55	51.87	−0.90	0.28	0.23	162
	10 12 51.82	40 39 04.18	–	6.44	–	–	–	–	–	–
	10 12 51.74	40 39 01.82	186.33	93.45	−0.64	57.87	−0.88	0.52	0.36	20
1125+327	11 28 02.61	32 30 50.16	83.68	68.59	−0.18	–	–	0.46	0.30	8
	11 28 02.44	32 30 46.54	–	0.99	–	–	–	–	–	–
	11 28 02.35	32 30 44.95	115.58	76.77	−0.38	–	–	0.58	0.41	34
	11 28 02.32	32 30 44.47	53.80	32.30	−0.47	–	–	0.38	0.32	64
1236+327	12 39 09.18	32 30 27.67	413.42	138.84	−1.01	–	–	0.47	0.29	93
	12 39 09.06	32 30 27.42	5.01	–	–	–	–	0.18	0.10	19
	12 39 09.00	32 30 26.94	122.41	–	–	–	–	0.74	0.25	47
	12 39 08.95	32 30 26.51	166.90	80.64	−0.68	–	–	0.31	0.16	82
1334+417	13 36 26.54	41 31 11.54	151.45	69.09	−0.73	–	–	0.48	0.25	133
	13 36 26.52	41 31 11.95	125.05	–	–	–	–	0.93	0.49	135
	13 36 26.20	41 31 15.46	58.22	44.12	−0.26	–	–	0.29	0.13	148
1542+323	15 44 48.43	32 08 44.06	303.42	140.71	−0.71	–	–	0.37	0.19	161
	15 44 48.33	32 08 46.13	404.75	164.80	−0.83	–	–	0.40	0.17	152
1723+406	17 25 16.34	40 36 42.15	97.98	42.75	−0.77	–	–	0.30	0.06	174
	17 25 16.33	40 36 43.48	322.92	79.46	−1.30	–	–	0.82	0.27	180
	17 25 16.21	40 36 39.04	351.39	110.64	−1.07	–	–	0.52	0.25	65

Description of the columns:

- Col. (1): source name in the IAU format;
- Col. (2): component right ascension (J2000) as measured at 1.7 GHz;
- Col. (3): component declination (J2000) as measured at 1.7 GHz;
- Col. (4): MERLIN flux density (mJy) at 1.7 GHz obtained using JMFIT;
- Col. (5): VLA flux density (mJy) at 4.9 GHz obtained using JMFIT;
- Col. (6): spectral index between 1.7 and 4.9 GHz calculated using flux densities in Cols. (4) and (5);
- Col. (7): VLA flux density (mJy) at 8.4 GHz obtained using JMFIT;
- Col. (8): spectral index between 4.9 and 8.4 GHz calculated using flux densities in Cols. (5) and (7);
- Col. (9): deconvolved component major axis angular size at 1.7 GHz obtained using JMFIT;
- Col. (10): deconvolved component minor axis angular size at 1.7 GHz obtained using JMFIT;
- Col. (11): deconvolved major axis position angle at 1.7 GHz obtained using JMFIT.

was proposed by Hatziminaoglou et al. (2001) – hereafter HSE (see also Siemiginowska et al. 1996; Siemiginowska & Elvis 1997; Janiuk et al. 2004). According to their model, galaxies spend the greater part of their lifetime (∼70%) in a "quiescent" state and ∼30% in an active state. RB97 do not investigate the physical mechanism that drives the short and frequent outbursts of activity in RLAGNs, but as suggested by Begelman (1999) their model can be combined with that of HSE who predict that, since the length of the active phase of an AGN as well as the timescale of activity re-occurrence is determined by the square of the mass of the SMBH, it follows that the length of an active phase *can* be as short as 10^5 years which, as indicated above, is typical for MSOs. Based upon the relationship given by HSE, this corresponds to a SMBH mass of ∼10^8 $M_\odot$. It is to be noted that, according to Oshlack et al. (2002) and Woo & Urry (2002), the range of SMBH masses residing in the centres of RLAGNs is very wide: 2×10^6 $M_\odot$ − 7×10^9 $M_\odot$.

This corresponds to a range of 7 orders of magnitude for allowable timescales for the duration of an active phase. Thus, the theory of thermal-viscous instabilities in the accretion disks of AGNs can be used to explain the existence of a very wide range of timescales of activity periods in RLAGNs. Eventually, this translates to a wide range of linear sizes starting from CSOs through MSOs up to the very extended, old LSOs which, if their sizes exceed 1 Mpc, are termed Giant Radio Galaxies (see e.g. Lara et al. 2001).

6. Summary and conclusions

The compactness of MSOs is interpreted as a direct consequence of their "youth". They are believed to be the precursors of larger/older objects and so eventually become LSOs. It is unclear whether *all* young sources actually evolve to become very extended objects. Some of them may be short-lived phenomena and can leave the main evolutionary track earlier because of a
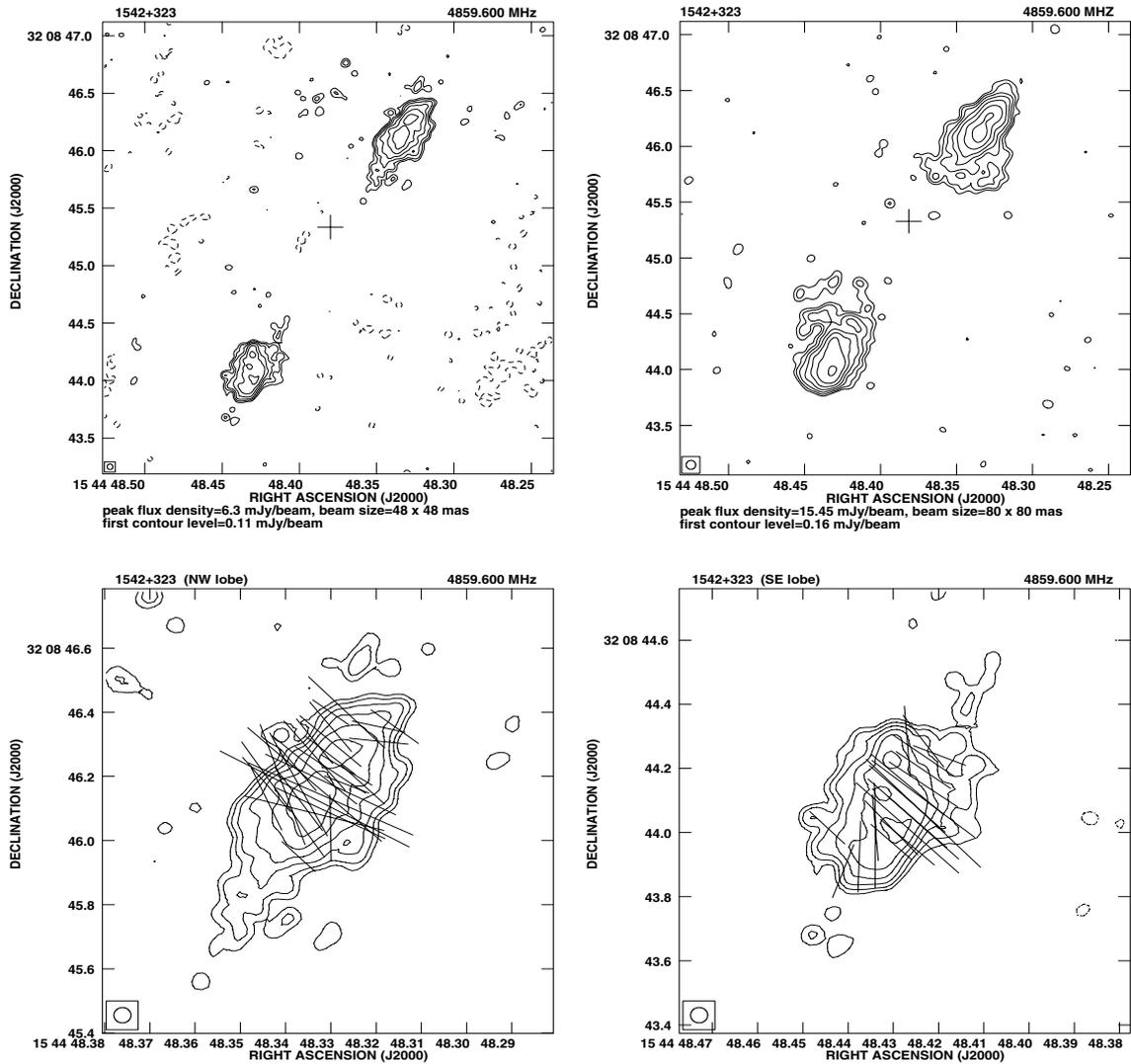
Fig. 4. MERLIN polarisation map of 1542+323 resulting from 12-h observation at 4.9 GHz (*upper left*). Combined MERLIN and VLA polarisation map of 1542+323 at 4.9 GHz (*upper right*). Lower panels show enlarged lobes of MERLIN-only map. Contours increase by a factor 2 and the first contour level corresponds to ≈3σ. Polarisation line of 1″ amounts to 1.33 mJy/beam for all maps. Crosses indicate the position of an optical object found using the SDSS/DR3.

lack of stable fuelling. Theoretical predictions made by RB97 combined with the model given by HSE allow for short periods of activity provided that the mass of the central SMBH is sufficiently low. The main goal of this study was to search for relic sources among those with subgalactic sizes. Finding examples of RLAGNs in which the energy transport has switched off early so that they have become compact faders would provide evidence that the scenario outlined above is plausible i.e. the activity of a RLAGN could decline at *any* stage of its evolution.

A new sample of weak CSS sources has been established and the sources observed to see if the evolutionary track for strong radio sources could be applied to weak ones. In this paper 6 sources from the sample which, based on a MERLIN 5-GHz snapshot survey seemed to be good candidates for "dying" MSOs, have been studied. Only one of them, 1542+323, possibly appears to be a fader. The other five sources show no obvious signs of being switched off.

References

Alexander, P., & Leahy, J. P. 1987, MNRAS, 225, 1

Arshakian, T. G., & Longair, M. S. 2000, MNRAS, 311, 846

Augusto, P., Browne, I. W. A., & Wilkinson, P. N. 1998, Ap&SS, 261, 261

Becker, R. H., White, R. L., & Edwards, A. L. 1991, ApJS, 75, 1

Begelman, M. C. 1999, The Most Distant Radio Galaxies, Proceedings of the colloquium, Amsterdam, 15−17 October 1997, ed. H. J. A. Röttgering, P. N. Best, & M. D. Lehnert, Royal Netherlands Academy of Arts and Sciences, 173 [arXiv:astro-ph/9712107]

Bennett, A. S. 1962, MmRAS, 68, 163

Best, P. N., Bailer, D. M., Longair, M. S., & Riley, J. M. 1995, MNRAS, 275, 1171

Browne, I. W. A., Wilkinson, P. N., Patnaik, A. R., & Wrobel, J. M. 1998, MNRAS, 293, 257

Cordey, R. A. 1987, MNRAS, 227, 695

De Breuck, C., van Breugel, W., Röttgering, H. J. A., & Miley, G. 2000, A&AS, 143, 303

Douglas, J. N., Bash, F. N., Bozyan, F. A., Torrence, G. W., & Wolfe, C. 1996, AJ, 111, 1945

Fanaroff, B. L., & Riley, J. M. 1974, MNRAS, 167, 31

Fanti, R., Fanti, C., Schilizzi, R. T., et al. 1990, A&A, 231, 333

Fanti, C., Fanti, R., Dallacasa, D., et al. 1995, A&A, 302, 317

Fanti, C., Pozzi, F., Dallacasa, D., et al. 2001, A&A, 369, 380

Feretti, L., Giovannini, G., Gregorini, L., Parma, P., & Zamorani, G. 1984, A&A, 139, 55

Ghisellini, G., Haardt, F., & Matt, G. 2004, A&A, 413, 535

Giovannini, G., Feretti, L., Gregorini, L., & Parma, P. 1988, A&A, 199, 73

Goldshmidt, O., & Rephaeli, Y. 1994, ApJ, 431, 586

Gopal-Krishna, & Wiita, P. J. 2000, A&A, 363, 507

Hatziminaoglou, E., Siemiginowska, A., & Elvis, M. 2001, ApJ, 547, 90 (HSE)

Jamrozy, M., Klein, U., Mack, K.-H., Gregorini, L., & Parma, P. 2004, A&A, 427, 79

Janiuk, A., Czerny, B., Siemiginowska, A., & Szczerba, R. 2004, ApJ, 602, 595

Kaiser, C. R., & Cotter, G. 2002, MNRAS, 336, 649

Komissarov, S. S., & Gubanov, A. G. 1994, A&A, 285, 27

Kunert, M., Marecki, A., Spencer, R. E., Kus, A. J., & Niezgoda, J. 2002, A&A, 391, 47 (Paper I)

Lara, L., Cotton, W. D., Feretti, L., et al. 2001, A&A, 370, 409

Liu, R., Pooley, G. G., & Riley, J. M. 1992, MNRAS, 257, 545

Lonsdale, C. J., & Morison, I. 1983, MNRAS, 203, 833

Machalski, J., & Condon, J. J. 1983, AJ, 88, 143

Machalski, J. 1998, A&AS, 128, 153

Murgia, M., Fanti, C., Fanti, R., et al. 1999, A&A, 345, 769

Oshlack, A. Y. K. N., Webster, R. L., & Whiting, M. T. 2002, ApJ, 576, 81

Owsianik, I., & Conway, J. E. 1998, A&A, 337, 69

Owsianik, I., Conway, J. E., & Polatidis, A. G. 1998, A&A, 336, L37

Patnaik, A. R., Browne, I. W. A., Wilkinson, P. N., & Wrobel, J. M. 1992, MNRAS, 254, 655

Peacock, J. A., & Wall, J. V. 1982, MNRAS, 198, 843

Polatidis, A. G., & Conway, J. E. 2003, PASA, 20, 69 [arXiv:astro-ph/0212122]

Readhead, A. C. S., Taylor, G. B., Xu, W., et al. 1996, ApJ, 460, 612

Reynolds, C. S., & Begelman, M. C. 1997, ApJ, 487, L135 (RB97)

Richstone, D., Ajhar, E. A., Bender, R., et al. 1998, Nature, 395, A14

Röttgering, H. J. A., Lacy, M., Miley, G. K., Chambers, K. C., & Saunders, R. 1994, A&AS, 108, 79

Saikia, D. J., Jeyakumar, S., Salter, C. J., et al. 2001, MNRAS, 321, 37

Saikia, D. J., Thomasson, P., Spencer, R. E., et al. 2002, A&A, 391, 149

Siemiginowska, A., Czerny, B., & Kostyunin, V. 1996, ApJ, 458, 491

Siemiginowska, A., & Elvis, M. 1997, ApJ, 482, L9

Slee, O. B., Roy, A. L., Murgia, M., Andernach, H., & Ehle, M. 2001, AJ, 122, 1172

Snellen, I. A. G., Schilizzi, R. T., Miley, G. K., et al. 1999, NewAR, 43, 675

Snellen, I. A. G., Schilizzi, R. T., Miley, G. K., et al. 2000, MNRAS, 319, 445

Spencer, R. E., McDowell, J. C., Charlesworth, M., et al. 1989, MNRAS, 240, 657

Tschager, W., Schilizzi, R. T., Röttgering, H. J. A., et al. 2003, A&A, 402, 171

Thomasson, P., Saikia, D. J., & Muxlow, T. W. B. 2003, MNRAS, 341, 91

Vigotti, M., Grueff, G., & Perley, R. 1989, AJ, 98, 419

White, R. L., Becker, R. H., Helfand, D. J., & Gregg, M. D. 1997, ApJ, 475, 479

Wilkinson, P. N., Browne, I. W. A., Patnaik, A. R., Wrobel, J. M., & Sorathia, B. 1998, MNRAS, 300, 790

Woo, J. H., & Urry, C. M. 2002, ApJ, 581, L5